NUCLEOSIDES & NUCLEOTIDES, 17(9-11), 1605-1611 (1998)

The Electronic Nature of the Aglycone dictates the Drive of the Pseudorotational Equilibrium of the Pentofuranose Moiety in C-Nucleosides

Ingrid Luyten[1], Jasenka Matulic-Adamic[2], Leo Beigelman[2] and Jyoti Chattopadhyaya[1*]

[1]Department of Bioorganic Chemistry, Box 581, Biomedical Centre, University of Uppsala, S-751 23 Uppsala, Sweden

[2]Ribozyme Pharmaceuticals Inc, 2950 Wilderness Place, Boulder, Colorado 80301, U.S.A

(E-mail: jyoti@bioorgchem.uu.se. Fax: +4618554495]

Abstract: We herein show for the first time that the specific electronic character of a C-aglycone dictates the thermodynamic preference of the two-state N ⇆ S pseudorotational equilibrium to either N- or S-type sugar. As the electron-deficiency of the C-aglycone increases, a more favourable O4'(n) → σ*(C1'-C(sp2)) interaction results into anomeric stabilization as indicated by more positive ΔH° for the drive of the N ⇆ S equilibrium to more N-type sugar conformation with pseudoaxial aglycone. Alternatively, as the C-aglycone becomes more electron-rich, an unfavourable O4'(n) → σ*(C1'-C(sp2)) interaction results into anomeric destabilization as indicated by more negative ΔH° for the drive of the N ⇆ S equilibrium to more S-type sugar conformation with pseudoequatorial aglycone.

The unique structural characteristic of C-nucleosides which distinguishes them from the ordinary N-nucleosides is the precense of a carbon to carbon bond instead of a carbon to nitrogen bond between the aglycone and the sugar moieties[1]. Many C-nucleosides have been isolated as antibiotics and exhibit anticancer and/or antiviral activity[2]. We have recently shown[3u] by quantitation of the energetics of pD-dependent N ⇆ S pseudorotational equilibria of the pentofuranose moiety in C-nucleosides that the strength of the anomeric effect of each C-nucleoside is indeed aglycone-dependent[3h] and tunable[3u] depending upon the pD of the medium, due to the change in the aromatic character of its nucleobase. It was not however possible in those work[3h,u] to show directly how a specific electron-rich or electron-deficient character of a C-aglycone promotes the N ⇆ S pseudorotational equilibria of the constituent sugar! In this work, through a thermodynamic study of the N ⇆ S pseudorotational equilibria of the sugar moiety of 9 different C-nucleosides **1 - 9**[4] (note the exact numbering of atoms in the C-aglycones), we unambiguously

show that an electron-deficient C-aglycone drives the sugar to the N-type conformation, whereas an electron-rich C-aglycone pushes it to the S-type. Such an unprecedented straight-forward correlation also shades light, for the first time, on the unique nature of the sugar O4' lonepair participation to the sp^2 hybridized C-aglycone system (the anomeric effect).

The anomeric effect (*i.e.* ΔH° term)[3] of C-aglycones on the drive of the two-state N ⇆ S pseudorotational equilibrium in C-nucleosides consists of two counteracting contributions from (i) the stereoelectronic interaction, which places the aglycone in the pseudoaxial orientation, and (ii) the inherent steric effect of the nucleobase, which opposes the stereoelectronic component of the anomeric effect by its tendency to take up the pseudoequatorial orientation. The signs of the thermodynamic parameters in Table 1 are arbitrarily chosen[3] in such a way that the positive values indicate the drive of N ⇆ S equilibrium to N, whereas the negative values describe the drive toward S.

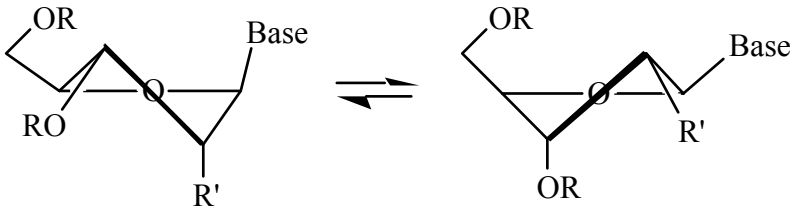

North sugar (C 3'-*endo*-C2'-*exo*), with pseudoaxial aglycone
Phase angle (P) : 0 ° Š P Š 36 °;
Puckering amplitude (Ψ_m) : 30Þ Š Ψ_m Š 46Þ

South sugar (C 2'-*endo*-C3'-*exo*), with pseudoequatorial aglycone
Phase angle (P) : 144 ° Š P Š 190 °;
Puckering amplitude (Ψ_m) : 30Þ Š Ψ_m Š 46Þ

We have classified the different C-aglycones in C-nucleosides **1 - 9** into three classes depending upon their electron-rich or electron-deficient character: (i) benzene derivatives, (ii) pyridine derivatives, and (iii) pyrimidine derivatives. We have tried to understand their electronic character by simply understanding the chemical reactivity of these aromatic rings[5,6] and correlate them with the experimental data on the thermodynamic preference of the N ⇆ S equilibrium.

(i) Benzene derivatives (1) - (3)

An examination of Table 1 shows that amongst the benzene derivatives **1 - 3**, the preference for the N-type conformation decreases in the following order: (**2**)[4b] (ΔH° = +0.4 kJ/mol) > (**1**)[4a] (ΔH°= -5.4 kJ/mol) > (**3**)[4c] (ΔH° = -7.3 kJ/mol). This decrease of the preference for the N-type sugar conformation as the C-aglycone changes from α-naphthyl in **2**, to phenyl in **1**, and to anilino in **3** can be understood from their inherent aromatic character: A simple comparison of the pK_as of phenol (9.99), α-naphthol (9.34) and β-naphthol (9.52) shows that the fused benzene rings in α-naphthol can delocalize the -OH lonepair more efficiently than phenol and β-naphthol. Similarly, a comparison of the basicity of the amino group in aniline (4.59), α-amino naphthalene (3.94) and β-amino naphthalene (4.20) confirms the unique aromatic nature of the fused naphthalene system vis-a-vis benzene. This is mainly owing to the more extensive delocalization of charges in naphthalene that makes α position more reactive than β position; this charge delocalization

capability also makes naphthalene more reactive than benzene. Interestingly, this relatively more efficient charge delocalization ability of the α-naphthyl moiety in (**2**) makes its sugar O4' lonepair (n) to delocalize to the σ* of the C1'-C(sp^2) fragment orbital in the gauche-gauche conformation more effectively than in phenyl in (**1**) [n(O4') → $\sigma^*_{(C1'\text{-}C(sp2))}$ interactions][7], thereby driving the sugar to the N-type conformation with the aglycone in the pseudoaxial orientation. This is also consistent with the fact that as the electron-density in the benzene ring of the anilino moiety in (**3**) increases compared with phenyl in (**1**), the delocalization ability of O4' lonepair to the C-aglycone decreases, driving the sugar conformation to the S-type sugar more successfully compared with the C1' phenyl aglycone. This is because the energy difference between the p-type orbital of O4' and the σ* of $C1'\text{-}C_{(sp2)}$ orbital is larger, as well as the overlap of the interacting orbitals is smaller, as the C-aglycone becomes more electron-rich, since the stabilization of the O4'(n) and $\sigma^*_{(C1'\text{-}C(sp2))}$ interaction is proportional to the square of the overlap between interacting orbitals and is inversely proportional to their energy difference[7].

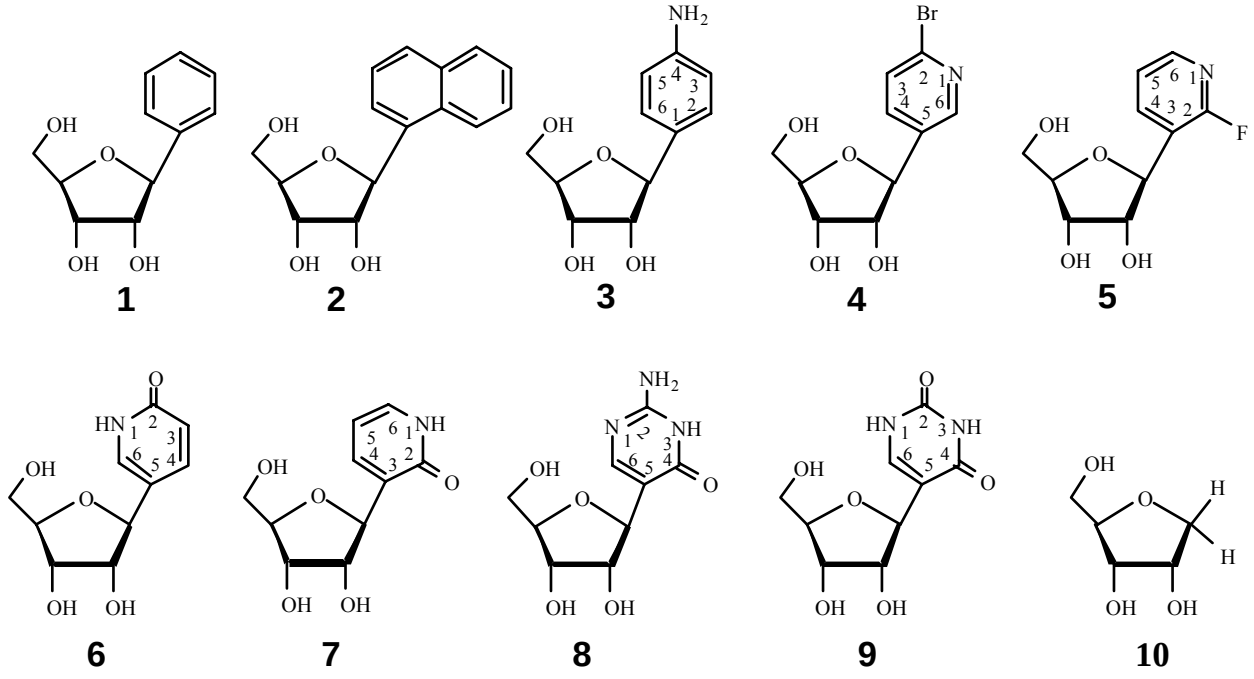

(ii) Pyridine derivatives (4) - (7)

In the pyridine series, a comparison of ΔH° of (**4**)[4d] (-4.4 kJ/mol) and (**6**)[4d] (-5.6 kJ/mol) with ΔH° of (**5**)[4e] (0.4 kJ/mol) and (**7**)[4e] (-0.1 kJ/mol) clearly shows that the substituent(s) in the pyridine ring as in **4** or **6**, respectively, has a comparable influence on n(O4') → $\sigma^*_{(C1'\text{-}C(sp2))}$ interactions as in the phenyl group in (**1**). This means that the influence of the electron-withdrawing group at para or meta/para position with respect to the sugar substituent is minimal. It is noteworthy that the effect of the nitrogen in the pyridine ring is more deactivating at positions 2 or 4 than at position 3 (*i.e.* the *meta* position with respect to pyridyl-nitrogen)[6], which is also clear from the relative rate of proton exchange for deuterium in the methyl groups of 2-, 3- and 4-methylpyridines (130 : 1 : 1810)[6b]. This situation however changes dramatically in the

pyridine derivatives with electron-withdrawing groups such as 2-fluoro pyridyl as in **5** or 2-pyridone group as in **7** (compared to **4** and **6**, respectively). The inductive (-I) effect of these ortho or ortho/meta substituents more effectively promotes the sugar O4' and the σ* of $C1'\text{-}C_{(sp2)}$ interactions because of more favourable orbital overlap as well as their relatively smaller energy difference, which is the driving force of the sugar to adopt a more N-type conformation.

Table 1: Dependence of the Thermodynamics of the Two State N ⧫;∅ S equilibrium upon the Electronic Nature≠ of the C-aglycone.

	Benzene-derivatives≠			Pyridine-derivatives≠				Pyrimidine-derivatives≠	
	(**1**)	(**2**)	(**3**)	(**4**)	(**5**)	(**6**)	(**7**)	(**8**)	(**9**)
ΔH°	-5.4 (0.8)	0.4(0.6)	-7.3 (1.0)	-4.4 (0.6)	0.4 (0.5)	-5.6 (0.9)	-0.1 (0.5)	-1.8 (0.3)	0.6 (0.2)
ΔS°	-8.7 (2.7)	2.7 (1.7)	-13.1(1.0)	-4.4 (2.0)	5.2 (1.7)	-7.4 (2.0)	0.7 (1.7)	-2.0 (1.1)	4.0 (1.1)
-TΔS°	2.6 (0.8)	-0.8 (0.5)	3.9 (0.8)	1.3(0.6)	-1.5 (0.5)	2.2 (0.6)	-0.2 (0.5)	0.4 (0.3)	-1.2 (0.3)
ΔG^{298};	-2.8 (0.5)	-0.4 (0.5)	-3.4 (0.4)	-3.1 (0.4)	-1.1 (0.1)	-3.4 (0.5)	-0.3 (0.2)	-1.4 (0.2)	-0.6 (0.1)
$\%S^{298}$	76	53	80	78	60	80	53	63	57
Actual AE*	-5.8	0.0	-7.7	-4.8	0.0	-6.0	-0.5	-2.2	0.3

The ΔH°, -TΔS° (at 298 K) and $\Delta G^{298}$are in kJ/mol. The standard deviations (σ) are in parentheses. For **8** and **9** , data are taken from ref 3u. ≠In this work, the steric contribution of the substituents in ΔH° could not be dissected because of the unavailability of the corresponding saturated system. *Actual anomeric effect (AE) was obtained by a simple subtraction of the ΔH° of the N ⧫;∅ S pseudorotational drive of 1-deoxy-β-D-ribopentofuranose (**10**) (ΔH° = 0.4 kJ/mol)[3a] from the ΔH° of a specific C-nucleoside.

(iii) Pyrimidine derivatives (8) and (9)

The incorporation of the second electron-withdrawing amide function in **7** (ΔH° = -0.1 kJ/mol) to give **9** (ΔH° = +0.6 kJ/mol) does not seriously change the relative strength of the anomeric effect. In contrast, the incorporation of the second electron-withdrawing amide function in **6** (ΔH° = -5.6 kJ/mol) to give **9** (ΔH° = +0.6 kJ/mol) considerably enhances the strength of the anomeric effect. This is again consistent with the above observation that the introduction of an electron-withdrawing ortho/meta substituent (with respect to sugar) in the pyridine is more important than at the para/meta position (with respect to sugar) to drive the N ⇆ S conformational equilibrium to the N-type sugar [compare also the ΔH° of (**4**) with (**5**), and (**6**) with (**7**)]. On the other hand, the drive of the N ⇆ S equilibrium can be reversed to more S-type conformation by substitution of the amide function in (**9**) (ΔH° = +0.6 kJ/mol) at the para/meta position (with respect to sugar) by an electron-donating amidine function to (**8**) (ΔH° = -1.8 kJ/mol).

The above examples clearly show that the information of the electronic character of the C-aglycone is indeed transmittable to drive the sugar confomation by altering the energy level of the σ* orbital of C1'-$C_{(sp2)}$ bond (E_2) with respect to the energy level of the p orbital (E_1) ($\Delta E = E_2 - E_1$) as well as their orbital overlap (S) potential (Anomeric stabilization ≈ $S^2 / \Delta E$)[7].

This is evident from the fact that as the electron-deficiency of the C-aglycone increases, we have a more favourable situation for the orbital overlap between the p orbital of O4' and the σ* orbital of the C1'-$C_{(sp2)}$ bond, which results into anomeric stabilization as indicated by more positive ΔH° for the drive of the N ⇆ S equilibrium to more N-type sugar conformation with pseudoaxial aglycone. Alternatively, as the C-aglycone becomes more electron-rich, we encounter an unfavourable situation for the orbital overlap between the p orbital of O4' and the σ* orbital of C1'-$C_{(sp2)}$ bond, which results into anomeric destabilization as indicated by more negative ΔH° for the drive of the N ⇆ S equilibrium to more S-type sugar conformation with pseudoequatorial aglycone.

Thus, this work shows that the ΔE as well as S of the interacting orbitals can indeed be influenced *predictably* by the nature of electron-deficient or electron-rich character of the C-aglycone.

Finally, the actual strength of the anomeric effect of various C-aglycones in (**1**) - (**9**) that promotes the drive of N ⇆ S equilibrium can however be obtained in a quantitative manner by a simple subtraction of the ΔH° of the N ⇆ S pseudorotational drive of 1-deoxy-β-D-ribopentofuranose (**10**) (ΔH° = 0.4 kJ/mol)[3a] from the ΔH° of a specific C-nucleoside (Table 1), which is shown in the last row of the Table 1.

In summary, we have developed a rational, along with our earlier works[3], that how the local structure of a polynucleotide can be governed by the electronic nature of aglycones (in addition to the base-base stacking, hydration, steric effects and inter- and intramolecular H-bonding), which have the unique ability to drive the sugar conformation in a very specific manner. Hence, the knowledge of the electronic nature of modified aglycones is important to understand how a new nucleobase would influence the local structure within a polynucleotide chain in the single-stranded, duplex or in the triplex form, since their conformational stabilities would dictate the success of gene-directed drugs (antisense or antigene therapy).

Table 2. The temperature-dependent vicinal coupling constants (Hz) of **1** - **9**[a].

		1[b]	**2**[c]	**3**[b]	**4**	**5**	**6**	**7**[b]	**8**	**9**
$J_{1'2'}$	278K	7.5	5.3	7.8	7.6	5.9	7.7	5.4	6.4	5.5
	358K	6.9	5.4	6.9	7.0	6.0	7.1	5.5	6.1	5.7
$J_{2'3'}$	278K	5.4	5.2	5.5	5.4	5.2	5.4	5.2	5.2	5.3
	358K	5.6	5.4	5.7	5.6	5.5	5.6	5.3	5.5	5.5
$J_{3'4'}$	278K	3.7	6.0	3.5	3.6	5.1	3.4	5.5	4.5	5.4
	358K	4.4	6.1	4.3	4.1	5.2	4.2	5.6	4.9	5.3

[a] error ± 0.1 Hz. Only $^3J_{HH}$ at the lowest and the highest temperature are tabulated, whereas they are available at several intermediate temperatures in 10 K steps. Note that the complete set of $^3J_{HH}$ between 278 and 358 K have been used in the calculation of thermodynamic quantities through pseudorotational analyses and van't Hoff plots. Tabulated coupling constants are the result of simulation and iteration procedure by DAISY program.[8] [b] $^3J_{HH}$ for **1, 3** and **7** could not be determined above 348 K because the signals for H2' and

H3'were buried under the watersignal. [c] $^3J_{HH}$ for **2** could not be determined above 338 K because the signals for H2' and H3' were buried under the watersignal.

Experimental Section

(A) ^{1}H-NMR spectroscopy

The C-nucleosides **1 - 9** were prepared using literature preocedures[4]. ^{1}H-NMR spectra were recorded at 500 MHz (Bruker DRX 500) in D_2O solution [1 mM for all compounds, δ_{CH_3CN} = 2.00 ppm as internal reference] between 278 K and 358 K at 10 K intervals. All spectra have been recorded using 64K data points and 32 scans. The accurate $^3J_{HH}$ (± 0.1 Hz) (Table 2) were obtained through simulation and iteration using DAISY program package[8] and have been used for the pseudorotational analyses.

(B) Conformational analysis with PSEUROT

The generalized Karplus equation[9b,c] used in the PSEUROT[9,10] program links coupling constants between vicinal protons to corresponding proton-proton torsion angles. The following λ substituent parameters were used for the substituents on H-C-C-H fragments : λ(C1') = λ(C3') = λ(C4') = λ(C2') = 0.62; λ(C5') = 0.68; λ(O4') = 1.27; λ(OH) = 1.26 and λ(C-aglycone) = 0.45[9c]. The PSEUROT analyses of temperature dependent $^3J_{HH}$ (278 K - 358 K, Table 2) of the sugar moieties of **1 - 9** were performed in either one or two steps in order to carefully examine the conformational hyperspace accessible to the N and S conformers: (i) Ψ_m(N) and Ψ_m(S) were assumed to be identical and they were kept fixed during the PSEUROT calculations, while P_N and P_S were optimized freely. (ii) When either the N-type or the S-type conformer is preferred by more than 65%, the geometry of the minor conformer was fixed while P and Ψ_m of the major conformer were optimized freely. Typically 5-10 separate PSEUROT calculations were performed in step (i) and 10 calculations in step (ii). To incorporate the error in the coupling constants (σ = 0.1 Hz), 1000 sets of randomly varied coupling constants (gaussian distribution) were generated and analyzed with a locally modified[11] version of the PSEUROT program[10] (Table 3 and the legend for specific description of the conformational spaces covered by the analyses). Typically, a total of 5000-20000 individual pseudorotational analyses were performed for each compound **1 - 9**. Some of the results were discarded due to (i) too large difference between a J_{calc} and J_{exp} (ΔJ_{max} = 0.5 Hz), (ii) too large overall rms in J_{HH} (rms_{max} = 0.3 Hz), (iii) $P_N < -40°$ or $P_N > 40°$, (iv) $P_S < 100°$ or $P_S > 180°$, or (v) $\Psi_m < 30°$ or $\Psi_m > 45°$ (see legend of Table 3). The total number of pseudorotational results that were used in the subsequent calculations of thermodynamic parameters is given in column 2 of Table 3. The mole fractions from the accepted pseudorotational analyses were used to construct van't Hoff plots. The averages of the slopes and the intercepts (Table 3) from the 3000-20000 van't Hoff plots were used to calculate ΔH° and ΔS° (and their errors) of the N ⇆ S sugar equilibrium of **1 - 9** (Table 3).

The free-energy ΔG^{298} values were calculated in two ways: (i) By taking the sum of ΔH° and -TΔS°. The standard deviation of ΔG^{298} is derived from the standard deviations of the ΔH° and -TΔS° values by the formula $\sigma=(\sigma_{\Delta H;}^2 + \sigma_{-T\Delta S;}^2)^{1/2}$ which gives a rather high error for ΔG^{298} because of the error propagation (and amplification) by the multistep procedure. (ii) From the average of the 3000-20000 individual $\ln(x_S / (1$

- x_S)) at 298K. This we refer to as $\ln_{av}(x_S / (1 - x_S))$ with its standard deviation [$\sigma \ln_{av}(x_S / (1 - x_S))$]. The free energies at 298 K, obtained by using the formula $\Delta G^{298} = -R * 0.298 * \ln_{av}(x_S / (1 - x_S))$, are presented in the last column of Tables 3 with their corresponding standard deviations in parentheses. The error of ΔG^{298} is then directly calculated using the formula $\sigma\Delta G^{298} = -R * 0.298 * \sigma \ln_{av}(x_S / (1 - x_S))$, which is smaller compared to the one obtained with the first method. However, the value of ΔG^{298} is not changed compared to the first approach.

Acknowledgements

We thank the Swedish Board for Technical Development and Swedish Natural Science Research (NFR) Council, Swedish Board for Technical Development (NUTEK), Sweden and the D. Collen Research foundation, Belgium for generous financial support. Thanks are due to the Wallenbergstiftelsen, Forskningsrådsnämnden, and University of Uppsala for funds for the purchase of 500 and 600 MHz Bruker DRX NMR spectrometers.

References

1. (a) Cortese, R.; Kammen, H. O.; Spengler, S. J. and Ames, B. N. *J. Biol. Chem.* **1974,** *249,* 1103. (b) Samuelsson, T.; Boren. T.; Johansen, T. I. and Lustig, F. *J. Biol. Chem.* **1988**, *263,* 13692.
2. (a) Suhadolnik, R. J. *Nucleoside Antibiotics,* Wiley-Interscience, New York **1970**; *Nucleosides as Biochemical Probes,* Wiley-Interscience, New York **1979**; Townsened L. B. in *Handbook of Biochemistry and Molecular Biology,* 3rd ed., (Fasman G. D. ed.), *Vol. 1,* p 271, CRC Press, Columbus, Ohio **1975** (b) Hanessian, S. and Pernet, A. G. *Adv. Carbohydr. Chem. Biochem.* **1976**, *33,* 111. (c) Daves, G. D. and Cheng, C. C. *Prog. Med. Chem.* **1976**, *13,* 303. (d) Buchanan J. G. *Forsch. Chem. Org. Naturst.* **1983**, *44* 243. (e) Hacksell, U. and Daves, G. D. *Prog. Med. Chem.* **1985**, *22,* 1. (f) There are other types of C-glycosyl natural products in which the aglycons are not nitrogen heterocycles. Some of these C-glycosyl compounds have shown anticancer activity. Daves G. D. *Acc. Chem. Res.* **1990**, *23,* 201.
3. (a) Plavec, J.; Tong, W.; Chattopadhyaya, J. *J. Am. Chem. Soc.* **1993**, *115*, 9734. (b) Plavec, J.; Garg, N.; Chattopadhyaya, J. *J. Chem.Soc., Chem. Commun.* **1993**, 1011. (c) Plavec, J.; Koole, L. H.; Chattopadhyaya, J. *J. Biochem. Biophys. Meth.* **1992**, *25,* 253. (d) Koole. L. H.; Buck, H. M.; Nyilas, A.; Chattopadhyaya, J. *Can J. Chem.* **1987**, *65*, 2089. (e) Koole, L. H.; Buck, H. M.; Bazin, H.; Chattopadhyaya, J. *Tetrahedron* **1987**, *43*, 2289. (f) Koole, L. H.; Plavec, J.; Liu, H.; Vincent, B. R.; Dyson, M. R.; Coe, P. L.; Walker, R. T.; Hardy, G. W.; Rahim, S. G.; Chattopadhyaya J. *J. Am. Chem. Soc.* **1992**, *114*, 9934. (g) Plavec, J.; Thibaudeau, C.; Viswanadham, G.; Sund, C.; Chattopadhyaya, J. *J. Chem. Soc., Chem. Comm.* **1994**, 781. (h) Thibaudeau, C.; Plavec, J.; Watanabe, K. A.; Chattopadhyaya, J. *J. Chem. Soc., Chem. Comm.* **1994**, 537. (i) Thibaudeau, C.; Plavec, J.; Garg, N.; Papchikhin, A.; Chattopadhyaya, J. *J. Am. Chem. Soc.* **1994**, *116*, 4038. (j) Plavec, J.; Thibaudeau, C.; Chattopadhyaya, J. *J. Am. Chem. Soc.* **1994**, *116,* 6558. (k) Thibaudeau, C.; Plavec, J.; Chattopadhyaya, J. *J. Am. Chem. Soc.* **1994**, *116*, 8033. (m) J. Plavec Ph.D. Thesis, Department of Bioorganic Chemistry, Uppsala University, Sweden, **1995**. (n) Plavec, J.; Thibaudeau, C; Chattopadhyaya, J. *Tetrahedron* **1995**, *51*, 11775. (p) Thibaudeau, C. ; Plavec, J. and Chattopadhyaya, J. *J. Org. Chem.* **1996**, *61*, 266. (q) Chattopadhyaya, J. *Nucl. Acids Symposium Series* **1996**, *35*, 111. (r) Plavec, J.; Thibaudeau, C. and Chattopadhyaya, J. *Pure and Applied Chemistry,* **1996**, 68, 2137. (s) Thibaudeau, C. and Chattopadhyaya, J. *Nucleosides & Nucleotides* **1997**, in press. (t) Thibaudeau, C. and Chattopadhyaya, J. *J. Org. Chem.*, **1996**, submitted. (u) Luyten, I.; Thibaudeau, C. and Chattopadhyaya, J. *Tetrahedron*, **1997**, in press.
4. (a) Matulic-Adamic, J.; Beigelman, L.; Portman, S.; Egli, M. and Usman, N. *J. Org. Chem.* **1996**, *61*, 3909.(b) Matulic-Adamic, J.; Karpeisky, A. M.; Gonzales, C.; Burgin, A. M.; Usman, N.; McSwiggen, J. A. and Beigelman, L. *Collection of Czech. Chem. Comm.* **1996**, *61,* S271. (c) Matulic-Adamic, J. and Beigelman, L.

Tetrahedron, **1996**, *37,* 6973. (d) Matulic-Adamic, J. and Beigelman, L. *Tetrahedron*, **1997**, 38, 1669. (e) Matulic-Adamic, J. and Beigelman, L. *Tetrahedron*, **1997**, 38, 203.

5. March, J. *Advanced Organic Chemistry, Reactions, Mechanism and Structure,* 4th ed., Wiley-Interscience, New York **1992**.
6. (a) Acheson, R. M. *An Introduction to the Chemistry of Heterocyclic Compounds,* Wiley-Interscience, New York **1976**. (b) Parkam, W. E. and Olsen, P. E., *Tetrahedron* **1973**, 4783.
7. Pinto, B. M. and Leung, R. Y. N. in *The Anomeric Effect and Associated Stereoelectronic Effects,* Ed. Thatcher, G. R. J., Am. Chem. Soc., Washington, DC **1993**, p 126.
8. DAISY, Spin Simulation Program, provided by Bruker, was used with 7 spins systems.
9. (a) De Leeuw, F. A. A. M. and Altona, C. *J. Comp. Chem.* **1983**, *4,* 428 and PSEUROT, QCPE program No 463. (b) Diez, E.; Fabian, J. S.; Guilleme, J.; Altona, C. and Donders, L.A. *Mol. Phys.* **1989**, *68,* 49. (c) Donders, L. A.; de Leeuw, F. A. A. M. and Altona, C. *Magn. Reson. Chem.* **1989**, *27,* 556. (d) Altona, C.; Ippel, J.H.; Hoekzema, A. J. A. W.; Erkelens, C.; Groesbeek, G.; Donders, L.A. Magn. Res. Chem. **1989**, *27*, 564. 3 (e) Altona, C., Francke, R., de Haan, R, Ippel, J.H., Daalmans, G.J., Westra, Hoekzema, A. J. A. and van Wijk, J. *Magn. Res. Chem.* **1994**, *32*, 670.
10. Altona, C.; Sundaralingam, M. *J. Am. Chem. Soc.* **1972**, *94,* 8205; *ibid* **1973**, *95*, 233..
11. Our modification of the PSEUROT v.5.4 program (ref 8) is intended to make it possible to evaluate and assess the propagation of errors from the experimental J_{HH} throughout the PSEUROT calculations as well as throughout subsequent treatment of the obtained data. Our modified program has retained all features of the original PSEUROT program, all changes are additions. The estimated error, expressed as standard deviation (σ), for each J_{HH} is entered to the program as well as the desired number of sets of randomly varied J_{HH}s to be generated and subsequently analyzed by pseudorotational analyses. Typically, 1000 data sets are generated and individually analyzed. Each set of 'experimental data' will contain randomly varied J_{HH}s but over all the data sets, each J_{HH} is normally distributed around its experimental value with the given σ. The output from our modified program consists of statistical data (average, σ and skew of the calculated geometrical parameters and mole fractions as well as of the generated J_{HH}s) and results from all the individual pseudorotational analyses (the calculated geometrical parameters and mole fractions). It is also possible to discard results which fall outside given ranges (J_{calc}-J_{exp}, rms in J_{HH}, P_N, P_S, $\Psi_m(N)$ and $\Psi_m(S)$).

Table 3. Pseudorotational analyses of temperature-dependent $^3J_{HH}$ (from 278 to 358K)[a] and determination of Thermodynamics of the Two State N ⇆ S Equilibrium for C-nucleosides **1** - **9**

	Total number of PSEUROT analysis*	**Ψ_m constrained analyses in PSEUROT[b, d]**		**P_N and Ψ_m(N) constrained analyses in PSEUROT[c, d]**		**Slopes and intercepts of various van't Hoff plots from $\ln(X_S/X_N)$ vs $1000/T$[e]**		**Thermodynamics of N ⇆ S Equilibrium from van't Hoff plots[e,f]**			**Thermodynamics of N ♦,∅ S Equilibrium from the average populations[g]**
		P_N	P_S	P_S	Ψ_m(S)	average slopes (σ)	average intercepts (σ)	ΔH° (σ)	-TΔS° (σ)	ΔG^{298} = (ΔH° -TΔS°)	ΔG^{298} = -0.298*R$\ln_{av}$ ($x_S/(x_N)$)
1	16120	-40° - 40°	122° - 140°	121° - 139°	30° - 45°	0.66 (0.10)	-1.00 (0.28)	-5.4 (0.8)	2.6(0.8)	-2.8 (1.1)	-2.8 (0.5)
2	3903	0° - 29°	122° - 127°			-0.05 (0.07)	0.32 (0.25)	0.4 (0.6)	-0.8(0.5)	-0.4 (0.8)	-0.4 (0.5)
3	14536	-40° - 40°	122° - 138°	122° - 139°	31° - 45°	0.88 (0.12)	-1.57(0.31)	-7.3 (1.0)	3.9 (0.8)	-3.4 (1.3)	-3.4 (0.4)
4	15499	-40° - 40°	123° - 140°	123° - 140°	31° - 45°	0.53 (0.08)	-0.53 (0.25)	-4.4 (0.6)	1.3 (0.6)	-3.1 (0.8)	-3.1 (0.4)
5	7332	-25° - 39°	120° - 139°			-0.05 (0.06)	0.60 (0.20)	0.4 (0.5)	-1.5 (0.5)	-1.1 (0.7)	-1.1 (0.1)
6	14476	-40° - 16°	124° - 134°	124° - 141°	31° - 45°	0.68 (0.10)	-0.88(0.26)	-5.6 (0.9)	2.2 (0.6)	-3.4 (1.1)	-3.4 (0.5)
7	11405	-32° - 39°	112° - 145°			0.01 (0.06)	0.09 (0.20)	-0.1 (0.5)	-0.2 (0.5)	-0.3 (0.6)	-0.3 (0.2)
8	8938	-33° - 40°	120° - 144°			0.21 (0.04)	-0.17 (0.14)	-1.8 (0.3)	0.4 (0.3)	-1.4 (0.5)	-1.4 (0.2)
9	7141	-17° - 30°	120° - 133°			-0.11 (0.03)	0.65 (0.11)	0.6 (0.2)	-1.2 (0.3)	-0.7 (0.4)	-0.6 (0.1)

[a] $^3J_{HH}$ at 278 and 358 K are given in Table 2. [b] Assuming Ψ_m (N) = Ψ_m (S), we have kept Ψ_m (N) and Ψ_m (S) fixed to identical values in the range from 31° to 45° for **1**,°from 32° to 39° for **2**, from 37° to 43° for **3**, from 37° to 43° for **4**, from 32° to 42° for **5**, from 37° to 45° for **6**, from 32° to 45° for **7**, from 32° to 43° for **8**, from 32° to 39° for **9** and surveyed the conformational hyperspace in 1° steps during several PSEUROT optimizations which resulted in different populations of N and S conformers with their distinctive P_N and P_S. [c] P_N of the minor N-type conformers were fixed at $-40° \le P_N \le 40°$ in 20° steps with Ψ_m (N) being simultaneously fixed at 31°and 45° for **1**, at 37°and 43° for **3**, at 37° and 43° for 4 and at 37°and 45° for **6** during several PSEUROT optimizations which resulted in different populations of N and S conformers with their distinctive P_N and P_S. * For each of these PSEUROT[8,10] calculations the coupling constants were 1000 times randomized which resulted in different populations of N and S conformers with their distinctive P_N and P_S (see experimental section). [d] The error estimates of the PSEUROT analyses have been assessed in terms of ΔJ_{max} and r.m.s., both of which are reflecting the difference between J_{calc} and J_{exp} coupling constants. The number of successful PSEUROT analyses in column 2 are designated to those which were within the constrained values (see experimental section) as well as having a ΔJ_{max} and r.m.s. values smaller than 0.5 Hz and 0.3 Hz. [e] The populations of N and S pseudorotamers obtained through each of the above PSEUROT calculations at nine different temperatures, shown in column 2, are the basis for the identical number of van't Hoff plots, which in turn were used to calculate the average slope and intercept. [f]The average of the slopes and the intercepts derived from all van't Hoff plots given in the columns 7 and 8 were finally used to calculate the average ΔH°, -TΔS° (at 298K) and subsequently ΔG^{298} (kJ/mol^{-1}) of N ⇆ S equilibria of **1**. [g] ΔG^{298} calculated directly from the average logarithm $\ln_{av}$ (x_S/ (1- x_S)), by using the Gibbs equation $\Delta G^T = -(RT/1000)\ln_{av}$ (x_S/ (1- x_S)))with 1- $x_S = x_N$, R is the gas constant and T is the temperature. The standard deviations are in parentheses.